Branching relaxation pathways from the hot S_2 state of 8′-apo-β-caroten-8′-al

Yoonsoo Pang†[ab] and Graham R. Fleming*[ab]

Received 29th January 2010, Accepted 1st April 2010
First published as an Advance Article on the web 6th May 2010
DOI: 10.1039/c001322f

We present infrared and visible transient absorption measurements of 8′-apo-β-caroten-8′-al following one-photon excitation at 405 nm. An excess vibrational energy of ~4000 cm^{-1} in the S_2 state is created with 405 nm excitation. Relaxation from this vibronic region shows distinct relaxation pathways from those observed for 490 nm excitation which excites S_2 near its origin. Infrared and visible transient absorption measurements show long-lived transient signals that persist longer than 1 ns. These transient spectra are identical to those observed in previous two-photon excitation measurements at 1275 nm. Our results are consistent with at least two minima on the S_1 surface and a branched decay from hot S_2 molecules to at least two of these minima.

Introduction

Carotenoids have many roles in photosynthesis in nature. Carotenoids collect the blue-green region of sunlight and transfer it to chlorophylls,[1,2] and protect a reaction center from oxidative damage by quenching the singlet and triplet excited states of chlorophylls in an excess light condition.[3,4] Carotenoids are structural components of light-harvesting complexes in plants and photosynthetic bacteria,[5] so their conformational geometries and excited-state dynamics in protein structures are important to understand the photosynthesis.

The excited-state dynamics of carotenoids are exceedingly complex,[6–24] which implies a broad range of applications in nature. The electronic structure of carotenoids based on a C_{2h} symmetry of all-*trans*-polyene leads to the simple energy level scheme of the singlet excited states S_2 ($1^1B_u^+$) and S_1 ($2^1A_g^-$), and the ground state S_0 ($1^1A_g^-$).[6,7] The S_2 state populated by one-photon excitation rapidly relaxes to S_1 *via* a conical intersection[8,9] and the energy levels and dynamics of these singlet excited states have frequently been interpreted *via* the energy-gap law.[10–12] The calculation of Tavan and Schulten[13] which suggested that depending on conjugation length, a dark $1^1B_u^-$ state may lie between the $1^1B_u^+$ (S_2) and $2^1A_g^-$(S_1) states stimulated a number of experimental studies.[14–16] The $1^1B_u^-$ state has been proposed to play a role in the ultrafast S_2 to S_1 internal conversion. Once geometrical changes are allowed other expected states become accessible and in recent experimental studies on open-chain carotenoids and xanthophylls, Frank and co-workers showed that a state labeled S* with energy between S_2 and S_1 is an excited state with a twisted conformation compared to the ground state.[17,18]

Despite the extensive experimental and theoretical activity the excited-state dynamics of carotenoids are not fully understood.[16]

One challenging aspect of carotenoid photophysics is that excitation with differing amount of excess vibrational energy may result in differing relaxation pathways being followed.[25–29] For example, Polívka and co-workers compared excitation at 400 and 266 nm of zeaxanthin.[25] They observed the S* state with a 2.8–4.9 ps lifetime as a shoulder band at 510 nm regardless of the excitation wavelength, however the population in the S* state increased with increasing excess energy above the S_2 origin. In a second example, Larsen *et al.* suggested the existence of an $S^‡$ state from β-carotene which is formed directly from the S_2 state.[26] The $S^‡$ state was suggested to be a separate electronic state co-existing with the S_1 state with longer lifetimes (10 and 65 ps) than the S_1 state (10 ps). The relationship between the $S^‡$ and S* states is not clearly understood.[16]

The excited-state dynamics of 8′-apo-β-caroten-8′-al have been studied as a model carotenoid for highly symmetric carotenoids in a number of time-resolved experiments.[30–38] In our previous studies,[36,37] the excited-state dynamics of polarized carotenoids 8′-apo-β-caroten-8′-al and 7′,7′-dicyano-7′-apo-β-carotene were investigated by applying different pumping methods. One-photon excitation into the lowest vibrational level of the S_2 state and two-photon excitation direct to the S_1 state were compared. A model of two non-communicating minima on the S_1 potential energy surface was used to explain the distinct relaxation lifetimes and pathways following one- and two-photon excitation. Efficient formation of a long-lived species was observed following two-photon excitation, but this was absent with one-photon excitation. The long-lived species showed a similar infrared spectrum to that of a cation radical and gave a visible absorption band centered at 760 nm which is significantly blue-shifted from the absorption band of the cation radical.[39–42] A charge-transfer complex of a carotenoid and a solvent molecule was proposed as the nature of the long-lived species, although the possibility

[a] *Department of Chemistry, University of California, Berkeley, California 94720-1460, USA. E-mail: GRFleming@lbl.gov; Fax: +1510-642-6340; Tel: +1510-643-2735*
[b] *Physical Biosciences Division, Lawrence Berkeley National Laboratory, Berkeley, California 94720-1460, USA*
† Present address: Argonne National Laboratory, Chemical Sciences and Engineering Division, 9700 South Cass Ave, Argonne, IL 60493, USA.

of an unexcited carotenoid forming the complex with the excited molecule was also considered.[37]

In this study, we explore the excited state dynamics of 8′-apo-β-caroten-8′-al following one-photon excitation of S_2 with $\sim$4000 cm^{-1} of excess vibrational energy. Both time-resolved infrared and visible transient absorption spectroscopy are utilized.

Experimental methods

A Ti:sapphire amplifier system (Micra-5 oscillator and Legend Elite USP amplifier, Coherent) produces $\sim$35 fs, $\sim$1 mJ pulses centered at 810 nm with a 1 kHz repetition rate. Pump pulses ($\sim$50 fs, $<$0.5 μJ at sample position, 405 nm) were produced by doubling the amplifier output and compressing with a prism pair compressor. Mid-infrared probe pulses (100 fs, 2 μJ, tunable in 1250–3000 cm^{-1}) were produced by a difference frequency generation in a $AgGaS_2$ crystal between the signal and idler pulses of a near-infrared optical parametric amplifier (OPA).[43]

A time-resolved infrared spectrometer based on a MCT array detector (IR-6416, Infrared Systems) was used for transient infrared measurements.[36] A silicon photodiode attached to a double grating monochromator (DH10, Horiba Jobin Yvon) and probe pulses at 550 and 760 nm generated by a visible OPA (Coherent 9450) were used for visible transient absorption measurements.

8′-Apo-β-caroten-8′-al and all the solvents were purchased from Sigma-Aldrich and were used without further purification. Sample concentrations were 2.4 mM for infrared measurements and 75–600 μM for visible transient absorption measurements. A liquid sample cell of 250 μm thickness was used to recirculate the sample at ambient temperature.

Results and discussion

Vibronic structure

Steady-state absorption spectra of 8′-apo-β-caroten-8′-al in chloroform and cyclohexane solution are shown in Fig. 1 along with its molecular structure. The absorption spectrum in a nonpolar solvent cyclohexane shows three resolved vibronic bands at 487, 460, and 435 nm. These bands are assigned as the 0–0, 0–1, and 0–2 vibronic bands of the $S_0 \rightarrow S_2$ transition, respectively. There is a shoulder around 410 nm in the cyclohexane spectrum, which can be assigned as the 0–3 vibronic band. Higher vibronic bands of the S_2 state can be clearly resolved at low temperature as seen in the case of spheroidene and other open-chain carotenoids.[44] The vibronic structure in the absorption spectrum is missing in a polar solvent such as chloroform (n = 1.4458); the absorption band has λ_{max} = 475 nm, red shifted from the strongest 460 nm band in cyclohexane (n = 1.4262) due to the increase in solvent polarizability, calculated *via* the refractive index equation of $(n^2 - 1)/(n^2 + 2)$. The 405 nm excitation pulse used in this work will populate 0–3 or higher vibrational bands of the $S_0 \rightarrow S_2$ transition according to the absorption spectrum.

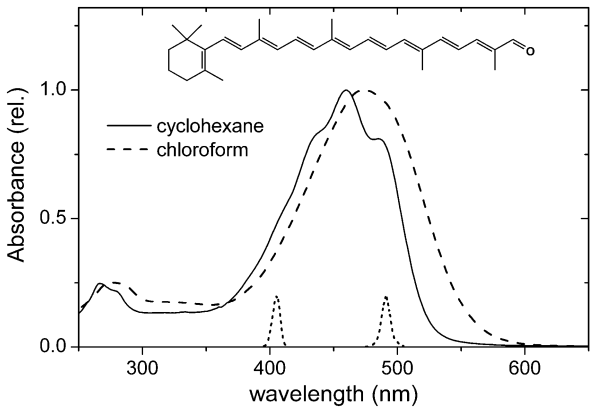

Fig. 1 Steady-state absorption spectra of 8′-apo-β-caroten-8′-al in chloroform and cyclohexane solution. The molecular structure of 8′-apo-β-caroten-8′-al is shown in the inset and the spectra of the 405 and 490 nm excitation pulses are shown as dotted lines.

Transient infrared absorption

Fig. 2 shows surface plots for the excited-state infrared absorption spectra of 8′-apo-β-caroten-8′-al in chloroform solution following 405 and 490 nm excitations. These plots were constructed from the difference infrared spectrum at each delay time. A strong and broad band around 1700 cm^{-1} in both spectra is the $\nu_{C=O}$ mixed with blue-shifted $\nu_{C=C}$ modes, and two medium-strong bands at 1550 and 1585 cm^{-1} are the

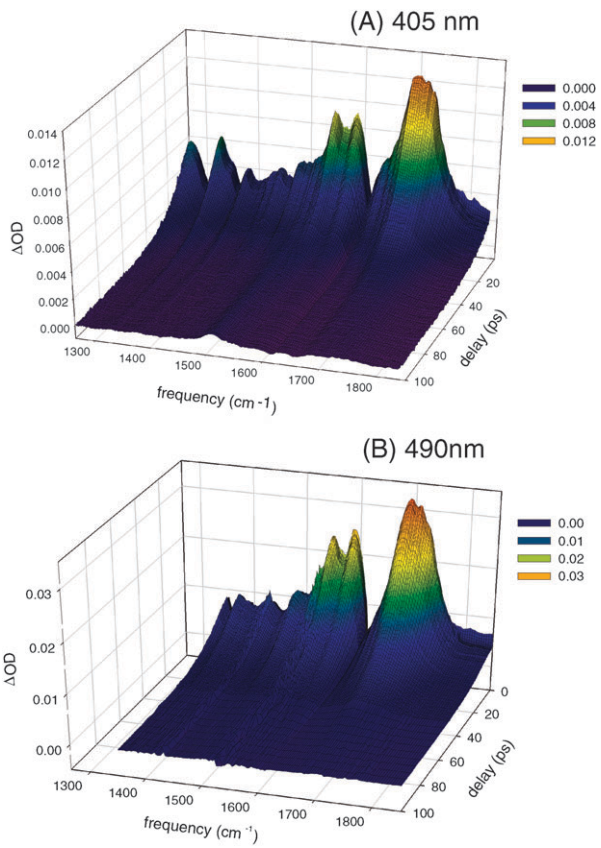

Fig. 2 Surface plots of excited-state infrared spectra of 8′-apo-β-caroten-8′-al in chloroform solution following (A) excitation at 405 nm and (B) excitation at 490 nm (reproduced from ref. 36).

$\nu_{C=C}$ modes. All these bands at early time delays in Fig. 2B are the vibrational bands in the S_1 state, from which a consistent S_1 lifetime of 19.4 ps is obtained with 490 nm excitation. The details of the vibrational assignment and the kinetics results with 490 nm excitation were given elsewhere where it was noted that the S_1 infrared bands are roughly 7 times stronger than the ground state bands making bleaches difficult to detect.[36] The short time (*e.g.* 1 ps) infrared spectrum with 405 nm excitation is very similar to that obtained with 490 nm excitation as seen in Fig. 3. However the small increase in amplitude between 1350 cm^{-1} and 1550 cm^{-1} in the 405 nm-excited spectrum is consistent with there being a small ($\sim$5%) amount of the infrared spectrum obtained *via* 1275 nm two-photon excitation mixed with the 490 nm one-photon excited spectrum. This suggests a branched relaxation to the two minima on the S_1 surface when S_2 possesses sufficient excess vibrational energy. However, an alternative explanation for the small difference seen in Fig. 3 is that the 405 nm spectrum simply reflects a 'hotter' population of molecules. The population of the S_1 state has completely decayed to the ground state by 100 ps when excitation at 490 nm is used. However, several peaks and bleaches with non-zero absorption values are clearly visible at 100 ps when the pump is at 405 nm as seen in Fig. 2A. The long-lived species seen with 405 nm excitation does not decay on a 1 ns time scale and clearly reveals an excitation wavelength dependence of the S_2 and S_1 excited-state dynamics in 8′-apo-β-caroten-8′-al.

Difference infrared absorption spectra taken from the surface plot of Fig. 2A and the kinetic traces of three infrared absorption bands of 8′-apo-β-caroten-8′-al following 405 nm excitation are shown in Fig. 4. All the infrared absorption bands in the 1–30 ps delay region come from the S_1 spectrum while the bands remaining after 100 ps come from a long-lived species which is not the relaxed S_0 state. The S_1 lifetime can be accurately determined for the bands centered at 1547, 1586, and 1699 cm^{-1} and exponential fits give a time constant of 17.1–18.4 ps, a little shorter than 19.4 ps obtained with one-photon excitation at 490 nm but similar to $\sim$17 ps obtained with two-photon excitation at 1275 nm. The strongest

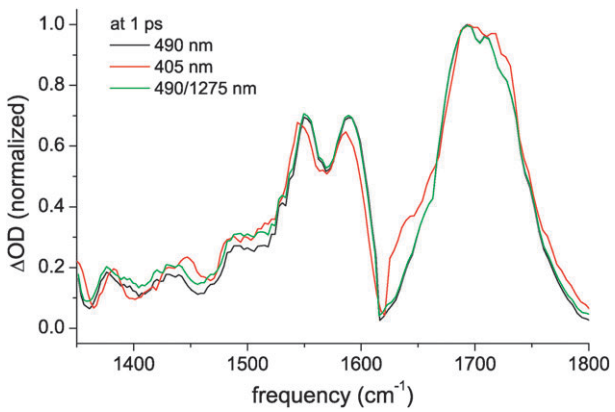

Fig. 3 Transient infrared spectra of 8′-apo-β-caroten-8′-al in chloroform solution following 405 nm (red) and 490 nm (black) excitations at 1 ps time delay. A constructed spectrum of 490 nm (95%) and two-photon excitation at 1275 nm (5%) is shown as a green line. All spectra are normalized to the carbonyl peak for comparison.

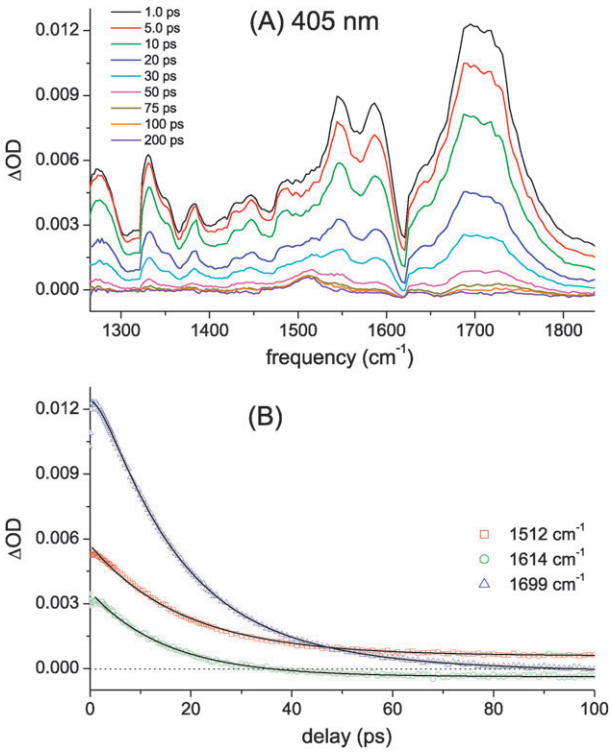

Fig. 4 (A) Transient infrared spectra of 8′-apo-β-caroten-8′-al in chloroform solution following 405 nm excitation taken from the surface plot in Fig. 2A and (B) kinetic traces of the $\nu_{C=C}$ and $\nu_{C=O}$ bands at 1512, 1614, and 1699 cm^{-1}. Exponential fits are shown as solid lines.

absorption band for the long-lived species at 1512 cm^{-1} showed a similar 18.4 ps decay along with 13% of a non-decaying component. The ground state bleach at 1614 cm^{-1} showed a 15.1 ps time constant along with about 10% of a non-decaying bleach component. The contribution of the long-lived species formation for excess energy (405 nm) one-photon excitation is $\sim$5% for comparison of infrared strengths between the strongest band of the S_1 state and a long-lived species. Referencing to the intensities of $\nu_{C=O}$ band at 1696 cm^{-1} (S_1 minimum), the $\nu_{C=C}$ band at 1510 cm^{-1} of a long-lived species with excess energy one-photon excitation at 405 nm is $\sim$15 times smaller compared to two-photon excitation results. The dynamics of this band is quite complex since it is affected by multiple processes including the instantaneous bleach upon excitation and the S_1 absorption created by the S_2 decay. All the exponential fit parameters are summarized in Table 1.

Table 1 Kinetics of the excited-state infrared absorption for 8′-apo-β-caroten-8′-al with 405 nm excitation

Frequency/cm^{-1}	a_1[a]	τ_1/ps	a_2[a]	τ_2/ps
1512	0.87	18.4 ± 0.1	0.13[b]	—
1547	1.00	17.8 ± 0.2		
1586	1.00	17.1 ± 0.2		
1614	1.00	15.1 ± 0.1	−0.10[b]	—
1699	1.00	18.4 ± 0.1		

[a] Amplitudes are in arbitrary units, and a positive one represents a decay and a negative one a rise. [b] Decay of these components cannot be measured in 1 ns delay time.

Comparison with two-photon excitation

The difference infrared spectra of 8′-apo-β-caroten-8′-al in chloroform measured following one-photon excitation at 405 nm and two-photon excitation at 1275 nm,[36] taken at 1 ns and 750 ps delay time, respectively, are compared in Fig. 5A and B. The infrared spectra of the long-lived species of 8′-apo-β-caroten-8′-al both with 405 nm and 1275 nm excitation are identical. The strong absorption band at 1510 cm^{-1}, the bleach of the ground state $\nu_{C=C,asym}$ mode at 1614 cm^{-1}, and the dispersive pattern of the $\nu_{C=O}$ mode in the 1640–1700 cm^{-1} range are very similar in both spectra. This confirms that the long-lived species seen with the excess vibronic energy excitation is the same as that found with two-photon excitation.[37] The calculated difference infrared spectrum[37] between the cation radical and the neutral molecule of 8′-apo-β-caroten-8′-al is plotted in Fig. 5C to show the similarities between the experiments and model. The cation radical model explains the several-fold increase in the infrared absorption strength of the mode around 1510 cm^{-1} observed in the transient infrared experiments. Such an increase was not seen from any other radical or conformational isomer in the ground state.[37]

Visible transient absorption

Transient absorption measurements with visible probe wavelengths can provide additional information about the excited-state processes following excitation at 405 nm. Kinetic traces of three transient absorption measurements following 405 nm excitation are shown in Fig. 6; the ground state recovery (GSR) probed at 405 nm, the $S_1 \rightarrow S_N$ excited state absorption (ESA) at 550 nm, and a long-lived species absorbing at 760 nm. The GSR probe shows an instrument-limited instant rise and decays with two time scales of 17.2 and 100 ps. The $S_1 \rightarrow S_N$ ESA shows a delayed rise (300–400 fs due to internal conversion from S_2 and vibrational relaxation from hot S_1) and more complex decay dynamics with three time scales: 2.3, 23.6, and 170 ps. A similar delayed rise was seen from the 550 nm probe of 8′-apo-β-caroten-8′-al following 490 nm excitation, however a single exponential decay with a 19.3 ps lifetime was seen at this wavelength for the lowest energy excitation.[36] The normalized trace of the $S_1 \rightarrow S_N$ ESA following 490 nm excitation is also shown in Fig. 6B for comparison.

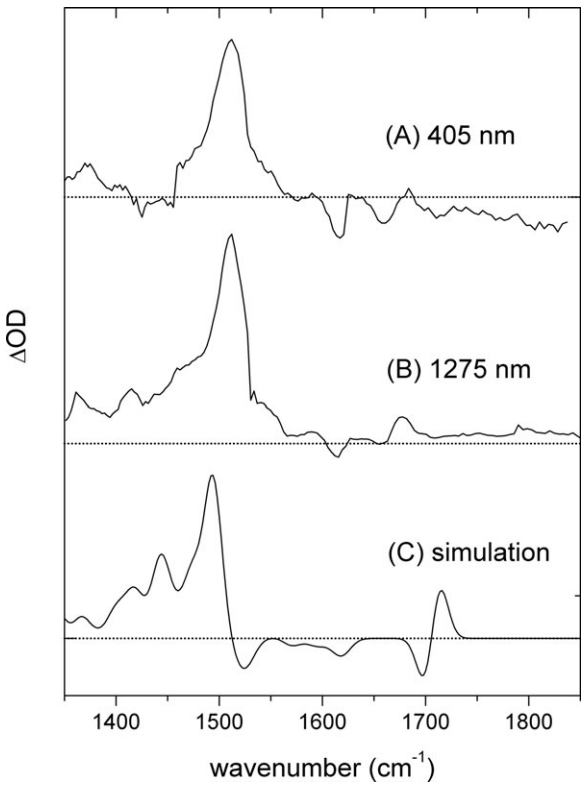

Fig. 5 Difference infrared spectra of 8′-apo-β-caroten-8′-al in chloroform solution measured with (A) one-photon excitation at 405 nm, (B) two-photon excitation at 1275 nm. The simulated difference (cation-neutral) infrared spectrum of 8′-apo-β-caroten-8′-al is shown in (C) for comparison. The zero absorption level is shown as a dotted line in each spectrum.

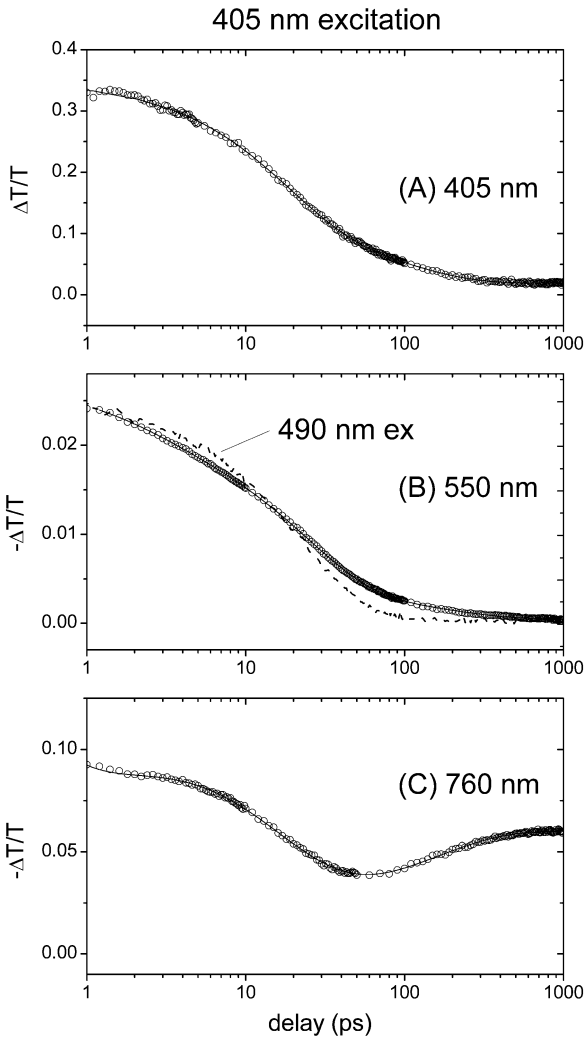

Fig. 6 Kinetic traces of the (A) ground state recovery probed at 405 nm, (B) $S_1 \rightarrow S_N$ excited state absorption at 550 nm, and (C) long-lived species absorption at 760 nm for 8′-apo-β-caroten-8′-al in chloroform solution following 405 nm excitation. Experimental results are shown as circles and exponential fits as lines. In panel (B), the kinetic trace of the $S_1 \rightarrow S_N$ excited state absorption at 550 nm following 490 nm excitation is shown with normalized intensities for comparison (dashed line).

Table 2 Kinetics of the transient absorption for 8′-apo-β-caroten-8′-al in chloroform solution with 405 nm excitation

a_1[a]	τ_1/ps	a_2[a]	τ_2/ps	a_3[a]	τ_3/ps
Ground state recovery at 405 nm					
		0.74	17.2 ± 0.3	0.26	100 ± 4
$S_1 \rightarrow S_N$ excited state absorption at 550 nm					
0.21	2.3 ± 0.1	0.67	23.6 ± 0.2	0.12	170 ± 6
Long-lived species absorption at 760 nm					
−0.23	2.5 ± 0.5	1.00	17.2 ± 0.7	−0.45	155 ± 7

[a] Amplitudes are in arbitrary units, and a positive one represents a decay and a negative one a rise.

The absorption band probed at 760 nm shows complex dynamics following 405 nm excitation. The 17.2 ps decay shows that a long wavelength tail of the S_1 ESA band is mixed with the long-lived species absorption at this wavelength and a single exponential rise with a 155 ps lifetime represents the formation of the long-lived species. However an additional component is required to improve the fit especially between 5–10 ps and in the 100 ps region. The third component shows a 2.5 ps lifetime which is similar to the short component in the $S_1 \rightarrow S_N$ ESA band. The fits are summarized in Table 2.

Overall, the excited-state dynamics of 8′-apo-β-caroten-8′-al in chloroform observed from visible transient absorption measurements show a similar 17–24 ps S_1 lifetime to the infrared results but also reveal a 155 ps rise for the 760 nm long-lived absorption band which was not detected in the infrared. The 100–170 ps decay component also appears in the S_1 ESA and GSR probe signals. The 155 ps rise time of the long-lived species seen with 405 nm excitation is quite similar to those observed with two-photon excitation at 1275 nm;[37] 142 ± 9 ps in the infrared and 166 ± 5 ps for the 760 nm probe wavelength. This strongly suggests the spectral identity of the long-lived species of 8′-apo-β-caroten-8′-al following one- (405 nm) and two-photon excitation (1275 nm). The lifetime of the long-lived absorption bands was not determined on a 1 ns scanning range in either case. The portion of the ground state population not recovered at 1 ns delay time is ~6% in the GSR measurement with 405 nm excitation. A fast relaxation channel to the long-lived species with ~2.5 ps time scale is also seen with 405 nm excitation and may originate from a hot S_1 state.

To confirm that the long-lived species is formed following one-photon excitation, the pump power dependence of the population of the S_1 state and the long-lived species were determined. The infrared absorption from the long-lived species is too weak to allow a reliable power dependence experiment, and we used the GSR signal probed at 405 nm instead. Fig. 7A shows the pump power dependence of the GSR signal at two delay times: at 17 ps the data mostly represent the S_1 population and at 100 ps the data represent the long-lived species population. Fits to both data sets give a linear dependence on pump power (1.11 ± 0.03 for 17 ps and 1.01 ± 0.05 for 100 ps).

Solvent and concentration dependence

The putative charge transfer complex of 8′-apo-β-caroten-8′-al created *via* two-photon excitation showed a dependence of its kinetics on solvent polarity. To investigate if such a solvent dependence carried over to the present results, infrared and visible transient absorptions of 8′-apo-β-caroten-8′-al in cyclohexane solution were measured following 405 nm excitation (data not shown). The S_1 state infrared spectrum of 8′-apo-β-caroten-8′-al in cyclohexane is very similar to the spectrum in carbon tetrachloride measured following one-photon excitation to the lowest level of S_2 (490 nm, see Fig. 9 in ref. 36). The infrared spectra of 8′-apo-β-caroten-8′-al in cyclohexane following 405 nm excitation show long-lived bands for $\nu_{C=C}$ at 1505 cm^{-1} and $\nu_{C=O}$ at ~1746 cm^{-1} and the visible transient absorption measurement at 760 nm shows a small absorption signal which lives longer than 1 ns but the quantum yield of this band at 760 nm is about 30 times smaller than in chloroform solution. This result is in accord with the two-photon data in showing that the second minimum on the S_1 potential surface has polarity dependent decay pathways.

To further understand the mechanism of the charge-transfer complex formation, we studied the concentration dependence of the transient absorption signal at 760 nm over the range 75–600 μM as shown in Fig. 7B. The absorption intensity of the long-lived transients measured at 1 ns delay time showed a linear dependence on this range. This excludes the possibility of the participation of an unexcited carotenoid molecule in the formation of the charge-transfer complex following one-photon

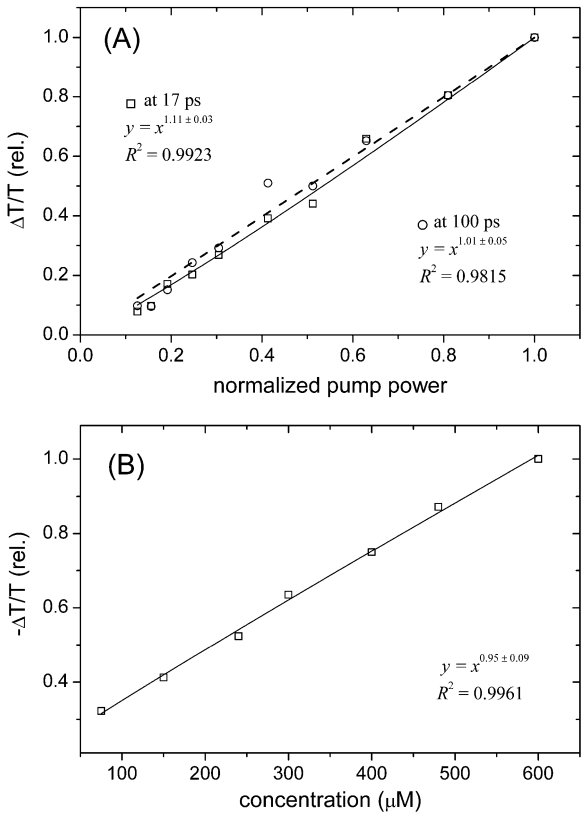

Fig. 7 (A) Pump-power dependence of the ground state recovery signal probed at 405 nm for 8′-apo-β-caroten-8′-al in chloroform following 405 nm excitation. Fits to data at 17 ps and at 100 ps delay both show one-photon behavior. (B) Sample concentration dependence of the long-lived species absorption probed at 760 nm for 8′-apo-β-caroten-8′-al in chloroform following 405 nm excitation.

excitation at 405 nm. From the identical infrared and visible transients of 8′-apo-β-caroten-8′-al following 405 nm and 1275 nm excitations, the charge-transfer complex formation with two-photon excitation at 1275 nm can be assumed to occur in a similar manner.

Relaxation pathways

When the S_2 state of 8′-apo-β-caroten-8′-al is excited near its origin a simple four state relaxation scheme $S_2 \rightarrow S_1$ (hot) $\rightarrow S_1 \rightarrow S_0$ suffices to explain the infrared- and visible-probe data. However, when substantial excess vibrational energy is initially deposited in S_2 ($\sim$4000 cm^{-1} in the present experiments) a branched scheme giving rise to distinct relaxation pathways is required. Both an S_1 state very similar to that obtained with 490 nm excitation, and a long-lived species similar to that obtained when S_1 is prepared directly *via* two-photon excitation at 1275 nm are seen. The simplest picture would then be that the vibrationally excited S_2 state can access both minima on the S_1 surface prepared in our previous work.[36] The yield of the long-lived species with 405 nm excitation is significantly smaller than with 1275 nm excitation, consistent with the S_1 infrared spectrum for 405 nm excitation strongly resembling the spectrum obtained with 490 nm excitation. Surface crossing from S_2 appears to occur significantly faster than vibrational equilibration within S_2 enabling access to a broader range of configurations in S_1 including the region accessed by direct two-photon excitation. Branching between multiple lower states from hot S_2 has been described for both β-carotene and zeaxanthin.[25,26] In the case of zeaxanthin the ratio of the S* state to the S_1 state increased with increasing excess energy in S_2.[25] In our case the fact that the S_1 region accessed by two-photon excitation is formed with considerable excess energy from the hot S_2 state presumably accounts for the new $\sim$2.5 ps component seen in the excited state absorption for 405 nm excitation, since the 1275 nm excitation does not provide excess vibrational energy to S_1.

In our earlier study of dynamics following two-photon excitation we suggested that the additional ground state bleach observed after S_1 decay may imply the involvement of a second, unexcited, carotenoid molecule.[37] However, being able to observe the long-lived transient with one-photon excitation enabled us to study the concentration dependence over a reasonable range. The finding that the 760 nm signal is strictly linear in carotenoid concentration over the 75–600 μM range leads us to conclude that this transient involves only a single carotenoid molecule which is an electron donor with a solvent molecule being an electron acceptor to create the cation radical-like spectrum observed in that work and the present study.

It is likely that the presence of an electron withdrawing group in 8′-apo-β-caroten-8′-al enables more complex dynamics than the non-polar carotenoids. For example Kopczynski *et al.* found a long-lived intramolecular charge transfer state in 8′-apo-β-caroten-8′-al which gives rise to stimulated emission at 890–900 nm on a long, strongly solvent dependent, time scale.[33] The lifetime of this state, however is too short to account for the long-lived visible and infrared bands observed here and in ref. 33.

Conclusions

The carotenoid 8′-apo-β-caroten-8′-al shows remarkably complex dynamics for the singlet excited states. There are at least 3 distinct regions of the S_1 surface: the region created *via* relaxation for the relaxed S_2, the region populated by direct two-photon excitation, and a proposed intramolecular charge transfer state. Excess vibrational energy in the S_2 state creates distinct relaxation pathways to generate a long-lived species which is not observed when population near the S_2 origin is created. The long-lived species observed following one-photon excitation at 405 nm shows an identical infrared spectrum and visible absorption band to those observed following two-photon excitation at 1275 nm which directly populates the S_1 state. This suggests that vibrationally hot S_2 molecules have access to the same region of the S_1 surface as is prepared by two-photon excitation. This pathway, however, has a significantly smaller yield than the pathway to the S_1 state typically observed after one-photon excitation. We hope that these results will stimulate electronic structure exploration of the multi-dimensional potential surfaces of these complex and fascinating molecules.

Acknowledgements

This research is based on work supported by the National Science Foundation under award CHE 0706468.

References

1 H. A. Frank and R. J. Cogdell, *Photochem. Photobiol.*, 1996, **63**, 257–264.
2 H. van Amerongen and R. van Grondelle, *J. Phys. Chem. B*, 2001, **105**, 604–617.
3 K. K. Niyogi, *Annu. Rev. Plant Physiol. Plant Mol. Biol.*, 1999, **50**, 333–359.
4 B. Demmig-Adams and W. W. Adams, *Nature*, 2000, **403**, 371–374.
5 H. Paulsen, in *The Photochemistry of Carotenoids*, ed. H. A. Frank, A. Young, G. Britton and R. J. Cogdell, Kluwer Academic Publishers, Dordrecht, 1999, pp. 123–135.
6 G. Orlandi, F. Zerbetto and M. Z. Zgierski, *Chem. Rev.*, 1991, **91**, 867–891.
7 T. Polívka and V. Sundström, *Chem. Rev.*, 2004, **104**, 2021–2071.
8 W. Fuß, Y. Haas and S. Zilberg, *Chem. Phys.*, 2000, **259**, 273–295.
9 M. Garavelli, P. Celani, F. Bernardi, M. A. Robb and M. Olivucci, *J. Am. Chem. Soc.*, 1997, **119**, 11487–11494.
10 R. Englman and J. Jortner, *Mol. Phys.*, 1970, **18**, 145–164.
11 K. F. Freed, *Acc. Chem. Res.*, 1978, **11**, 74–80.
12 V. Chynwat and H. A. Frank, *Chem. Phys.*, 1995, **194**, 237–244.
13 P. Tavan and K. Schulten, *Phys. Rev. B: Condens. Matter*, 1987, **36**, 4337–4358.
14 C. C. Gradinaru, J. T. M. Kennis, E. Papagiannakis, I. H. M. van Stokkum, R. J. Cogdell, G. R. Fleming, R. A. Niederman and R. van Grondelle, *Proc. Natl. Acad. Sci. U. S. A.*, 2001, **98**, 2364–2369.
15 G. Cerullo, D. Polli, G. Lanzani, S. De Silvestri, H. Hashimoto and R. J. Cogdell, *Science*, 2002, **298**, 2395–2398.
16 T. Polívka and V. Sundström, *Chem. Phys. Lett.*, 2009, **477**, 1–11.
17 H. Cong, D. M. Niedzwiedzki, G. N. Gibson and H. A. Frank, *J. Phys. Chem. B*, 2008, **112**, 3558–3567.
18 D. Niedzwiedzki, J. F. Koscielecki, H. Cong, J. O. Sullivan, G. N. Gibson, R. R. Birge and H. A. Frank, *J. Phys. Chem. B*, 2007, **111**, 5984–5998.
19 H. A. Frank, J. A. Bautista, J. Josue, Z. Pendon, R. G. Hiller, F. P. Sharples, D. Gosztola and M. R. Wasielewski, *J. Phys. Chem. B*, 2000, **104**, 4569–4577.

20 W. Wohlleben, T. Buckup, J. L. Herek and M. Motzkus, *ChemPhysChem*, 2005, **6**, 850–857.
21 P. Kukura, D. W. McCamant and R. A. Mathies, *Annu. Rev. Phys. Chem.*, 2007, **58**, 461–488.
22 T. Buckup, J. Hauer, J. Mohring and M. Motzkus, *Arch. Biochem. Biophys.*, 2009, **483**, 219–223.
23 A. Dreuw, *J. Phys. Chem. A*, 2006, **110**, 4592–4599.
24 D. Ghosh, J. Hachmann, T. Yanai and G. K. L. Chan, *J. Chem. Phys.*, 2008, **128**, 144117.
25 H. H. Billsten, J. X. Pan, S. Sinha, T. Pascher, V. Sundström and T. Polívka, *J. Phys. Chem. A*, 2005, **109**, 6852–6859.
26 D. S. Larsen, E. Papagiannakis, I. H. M. van Stokkum, M. Vengris, J. T. M. Kennis and R. van Grondelle, *Chem. Phys. Lett.*, 2003, **381**, 733–742.
27 S. Akimoto, I. Yamazaki, S. Takaichi and M. Mimuro, *Chem. Phys. Lett.*, 1999, **313**, 63–68.
28 D. Kosumi, K. Yanagi, T. Nishio, H. Hashimoto and M. Yoshizawa, *Chem. Phys. Lett.*, 2005, **408**, 89–95.
29 R. Nakamura, R. Fujii, H. Nagae, Y. Koyama and Y. Kanematsu, *Chem. Phys. Lett.*, 2004, **400**, 7–14.
30 H. Hashimoto, Y. Miki, M. Kuki, T. Shimamura, H. Utsumi and Y. Koyama, *J. Am. Chem. Soc.*, 1993, **115**, 9216–9225.
31 Z. F. He, D. Gosztola, Y. Deng, G. Q. Gao, M. R. Wasielewski and L. D. Kispert, *J. Phys. Chem. B*, 2000, **104**, 6668–6673.
32 Z. F. He, L. D. Kispert, R. M. Metzger, D. Gosztola and M. R. Wasielewski, *J. Phys. Chem. B*, 2000, **104**, 6302–6307.
33 M. Kopczynski, F. Ehlers, T. Lenzer and K. Oum, *J. Phys. Chem. A*, 2007, **111**, 5370–5381.
34 F. Ehlers, T. Lenzer and K. Oum, *J. Phys. Chem. B*, 2008, **112**, 16690–16700.
35 F. Ehlers, D. A. Wild, T. Lenzer and K. Oum, *J. Phys. Chem. A*, 2007, **111**, 2257–2265.
36 Y. Pang, M. A. Prantil, A. J. Van Tassle, G. A. Jones and G. R. Fleming, *J. Phys. Chem. B*, 2009, **113**, 13086–13095.
37 Y. Pang, G. A. Jones, M. A. Prantil and G. R. Fleming, *J. Am. Chem. Soc.*, 2010, **132**, 2264–2273.
38 S. Akimoto, I. Yamazaki, T. Sakawa and M. Mimuro, *J. Phys. Chem. A*, 2002, **106**, 2237–2243.
39 R. M. Han, Y. X. Tian, Y. S. Wu, P. Wang, X. C. Ai, J. P. Zhang and L. H. Skibsted, *Photochem. Photobiol.*, 2006, **82**, 538–546.
40 R. M. Han, Y. S. Wu, J. Feng, X. C. Ai, J. P. Zhang and L. H. Skibsted, *Photochem. Photobiol.*, 2004, **80**, 326–333.
41 J. P. Zhang, R. Fujii, Y. Koyama, F. S. Rondonuwu, Y. Watanabe, A. Mortensen and L. H. Skibsted, *Chem. Phys. Lett.*, 2001, **348**, 235–241.
42 G. G. Gurzadyan and S. Steenken, *Phys. Chem. Chem. Phys.*, 2002, **4**, 2983–2988.
43 A. J. Van Tassle, M. A. Prantil and G. R. Fleming, *J. Phys. Chem. B*, 2006, **110**, 18989–18995.
44 D. M. Niedzwiedzki, D. J. Sandberg, H. Cong, M. N. Sandberg, G. N. Gibson, R. R. Birge and H. A. Frank, *Chem. Phys.*, 2009, **357**, 4–16.

